The multi scenarios applicability of GNSS differential positioning technology in the remeasurement of observatory azimuth in China

Yufei He[1], Xudong Zhao[1], Suqin Zhang[1], Qi Li[1], Fuxi Yang[2], Shaopeng He[3], Pengkun Guo[3] and Jinping Zhou[1]

[1]Institute of Geophysics, China Earthquake Administration, Beijing, 100081, China
[2]Xinjiang Earthquake Administration, Urumqi, 830011, China
[3]Hebei Earthquake Administration, Shijiazhuang, 230071, China

Correspondence to: Xudong Zhao (zxd9801@163.com)

Abstract. The azimuth angle of geomagnetic observatory markers is crucial for ensuring the reliability of geomagnetic observation data, and its remeasurement constitutes a core task in observatory operations. The Geomagnetic Network of China comprises 46 geomagnetic observatories, most of which have been in operation for over ten years since their establishment. Thus, completing the azimuth remeasurement at these observatories has become an important mission. By comparing the precision, efficiency, and environmental adaptability of astronomical observation methods and GNSS differential positioning techniques for azimuth measurement, it is found that GNSS differential positioning technology is more suitable for the implementation of this task than traditional astronomical methods. After systematically investigating the multi scenarios in azimuth remeasurement at geomagnetic observatories based on GNSS differential positioning technology, the measurement schemes for five remeasurement scenarios are proposed, which can be applied to measurements under practical conditions such as unobstructed paths, restricted pathways, and single point deployments. Through field validations at the Hongshan, Quanzhou, and Yulin observatories, the feasibility of Scenario I (flat and clear line of sight) and Scenario II (alternative clear path available) is confirmed. Furthermore, a preliminary analysis was conducted on potential error sources in different scenarios, and a prioritized implementation sequence was established for stations that simultaneously meet the conditions of each retest scenario. This work provides a scalable technical solution for azimuth measurement in complex geomagnetic observatories environments.

1 Intruduction

The geomagnetic field, as a fundamental physical field of Earth, not only protects biological evolution but also serves as a key parameter in geoscientific exploration. Geomagnetic observatories, designed for long term continuous monitoring of geomagnetic variations (Jankowski and Sucksdorff, 1996), acquire seven components vector data—total intensity (F), horizontal component (H), declination (D), inclination (I), and Cartesian coordinates (X, Y and Z). These data are extensively applied in deep resource exploration, high precision navigation, and space environment monitoring (Lu et al., 2022; Lin et al.,

2023; Zhang et al., 2024a). Ensuring the precision and accuracy of absolute geomagnetic observations is of paramount importance (Zhang et al., 2024b).

It is essential to emphasize that the absolute measurement of the seven geomagnetic components at observatories is achieved through a collaborative system comprising relative recorders and absolute observation devices (St-Louis et al., 2024; Bracke et al., 2025). The relative recorders enable continuous monitoring with a sub second sampling rate, while the absolute observations calibrate baseline values periodically via manual or automated methods (currently focusing on D, I and F components twice weekly). The integration of both systems produces continuous absolute observation data with minute level temporal resolution and accuracy better than 1 nT (Zhang et al., 2016). Consequently, the frequency and precision of absolute observations directly determine baseline reliability, which in turn impacts the quality of final data—this represents the key technical bottleneck in enhancing the accuracy of absolute geomagnetic observations within the current monitoring framework.

The magnetic declination (D), defined as the angle between the true north and geomagnetic meridian, is particularly critical for practical applications such as oil drilling and navigation (Shi et al., 2008; Li et al., 2023). Currently, the measurement of magnetic declination (D) at geomagnetic observatories is primarily conducted using fluxgate theodolites instruments (abbreviated as DI instruments), in conjunction with the azimuth angle of the observatory's reference markers. Consequently, the accuracy of the azimuth angle is fundamentally vital to the reliability of these measurements.

The azimuth marker is one of the critical core facilities at geomagnetic observatories, and the azimuth angle, defined as the angle between the true north and line connecting the center of the observation pillar to the center of the marker, is also a vital parameter. Typically, the construction of azimuth markers requires long term stability (CEA, 2004). When feasible, the markers should ideally be engraved or built directly onto bedrock. The measurement of the azimuth angle is generally completed during the observatory's construction phase (Zhou et al., 1997; Xu et al., 2003; Yang et al., 2008; Wang et al., 2014). If the absolute observation chamber of the observatory has not yet been roofed, the azimuth angle can be directly measured at the center of the observation pillar using either astronomical observation methods (Ma, 1995; Cheng et al., 1996; Liu et al., 2020; Khanzadyan and Mazurkevich, 2021) or GNSS differential positioning technology (Yin et al., 2008; Zhou et al., 2009; Li et al., 2015; Yu et al., 2018). The azimuth marker and angle are put into service simultaneously with the commencement of the observatory's operations.

The construction of azimuth markers requires long term stability. However, over extended periods of operation at geomagnetic observatories, these markers may undergo displacement due to natural environmental changes or human induced disturbances. For instance, geological tectonic activities (e.g., earthquakes), crustal deformation, or subsurface fluid movements could shift observation pillars. Similarly, urban expansion—such as the construction of large scale facilities nearby, urban loading, or groundwater extraction—may lead to tectonic deformation, causing positional changes in the azimuth markers. Therefore, periodic remeasurements of the marker azimuth angles are essential in geomagnetic observatory operations to verify accuracy and promptly correct errors, thereby ensuring the reliability and precision of geomagnetic data. Azimuth angle remeasurement is a core procedure for maintaining data quality. Consequently, the operating guidelines of China geomagnetic observatory explicitly require the azimuth angle to be remeasured every 10 years, and if significant changes in the markers are detected,

additional assessments need to be conducted immediately (CEA, 2001). The Geomagnetic Network of China consists of 46 geomagnetic observatories, most of which have been in operation for over a decade since their establishment. Thus, completing azimuth remeasurement at these observatories has become an important task.

The study first provides a concise introduction to two methods for measuring marker azimuth angles, followed by a comparative analysis. It further examines multi scenarios applicability across diverse geomagnetic observatory environments and proposes five remeasurement schemes based on GNSS differential positioning technology. Field validations at multiple observatories demonstrate the frameworks' effectiveness, offering methodological references for azimuth remeasurement protocols.

2 Azimuth measurement methods

Currently, geomagnetic observatories in China mainly use two methods for azimuth measurement: the traditional astronomical observation method and the modern GNSS technology. Both methods can achieve high-precision measurement results.

2.1 Traditional astronomical observation method

The astronomical observation method is a measurement technique that determines the astronomical longitude, latitude, and azimuth of a ground point by observing the positions of celestial bodies (such as the Sun, Polaris, or other stars) and utilizing the relationship between their motion and the Earth's rotation. For traditional astronomical measurements, they are classified into 1 to 4 grades based on measurement accuracy, with the corresponding measurement accuracies being $0.5''$, $1.0''$, $5.0''$, and $10.0''$ respectively. In practical measurements, there are also various astronomical observation methods, including the Polaris hour angle method (suitable for grade 1-4 measurements), the solar hour angle method (for grade 4), the multi-star meridian hour angle method (for grade 3-4), the Zinger method (for grade 1-4), the solar altitude method (for grade 4), the multi-star altitude method (grade 1-4), and so on. The celestial bodies to be observed and the observation methods are selected according to the requirements of the measurement grade.

In the northern hemisphere, especially for China, which is located in the mid-low latitudes, Polaris has a declination close to $90°$ and is a brightness star, making it easy to observe. Therefore, the Polaris arbitrary hour angle method is often used to measure the astronomical azimuth. However, since Polaris is not exactly at the North Pole, the precise astronomical longitude and latitude of the observation must be known before measuring the astronomical azimuth (Liu et al., 2020). Here, we only briefly introduce the Polaris hour angle method. Figure 1 illustrates the angular relationships among the azimuth marker, celestial body, and true north in the horizontal coordinate system centered at observation point O. In this system: Z represents the zenith, M denotes the ground azimuth marker, S' is the projection of celestial body S onto the horizontal plane, P stands the north pole, N is the intersection point of the great circle passing through the zenith and the north pole with the horizon. A indicates the celestial body's azimuth angle, and θ signifies the horizontal angle between the celestial body and the marker. To determine the azimuth angle (a_{NM}) of OM, the following two steps are required: (a) measure the horizontal

angle θ between the celestial body and the marker; (b) record the observation time and calculate the celestial body's azimuth angle A. Finally, the azimuth angle a_{NM} can be derived as follows:

$$a_{NM} = A + \theta \quad (1)$$

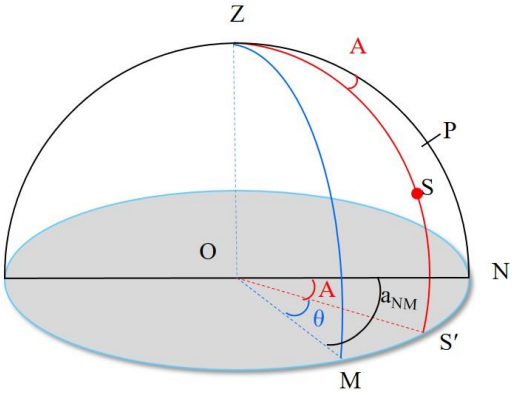

Figure 1: Spherical Diagram of Astronomical Azimuth

Figure 2 shows the spherical triangle ΔZPS used to calculate the azimuth of Polaris. Based on the altitude angle h of Polaris in the horizontal coordinate system, the latitude φ of the observation point, the declination δ of Polaris, and its hour angle t, the formula for calculating the celestial azimuth A (with the positive direction being eastward from north) can be derived using spherical trigonometry:

$$\mathrm{A} = \tan^{-1}\left(\frac{-\sin t}{\cos\varphi \tan\delta - \sin\varphi \cos t}\right) \quad (2)$$

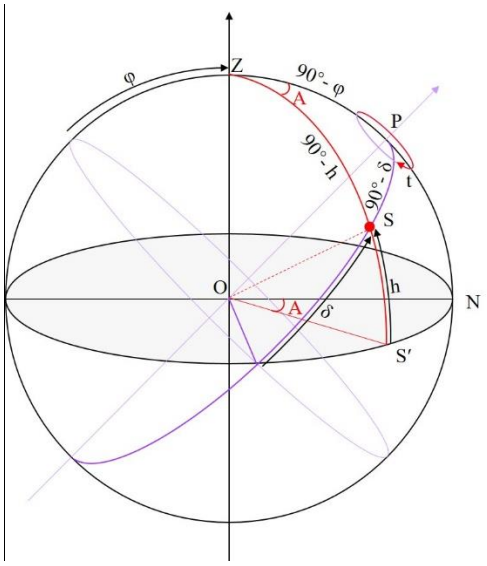

Figure 2: Spherical triangle for calculating the celestial azimuth

After obtaining the true northern azimuth of the Polaris through formula (2) and measuring its horizontal angle with the ground marker, the azimuth of the marker can be determined (SBQTS, 2000). In traditional astronomical observation methods, using the Sun as the observed celestial body can only achieve a relatively low accuracy level (Grade 4). For high-precision observations, especially to achieve Grade 1-2 astronomical observations, other celestial bodies are usually observed at night. Therefore, the measurement process is highly dependent on weather conditions and celestial body visibility; meanwhile, it also requires stable observation pillars and involves multi-period and multi-set observations.

2.2 Modern observation technology

Modern observation technologies for azimuth are primarily implemented via the Global Navigation Satellite System (GNSS), which encompasses satellite positioning systems such as the United States' GPS, Russia's GLONASS, Europe's Galileo, and China's BDS. Typically, GNSS employs two fundamental positioning methods: absolute positioning and relative positioning. The absolute method provides coordinates with lower precision, so it is used for navigation purposes; in contrast, the relative method delivers coordinates with higher precision and is therefore applied in positioning scenarios. Consequently, the GNSS differential positioning method is commonly utilized in azimuth measurement. The GNSS differential positioning method employs two stationary receivers (one serving as a base station and the other as a rover) to conduct synchronized prolonged continuous observations. Through post processing error elimination and baseline resolution, this technique acquires high precision three dimensional coordinates for both measurement points (A and B). Then transforming coordinates of A and B into a common planar coordinate system (e.g., UTM or local independent coordinate system) following IGS standards. Finally, the azimuth angle is derived from the planar coordinates of reference point (A) and target point (B), using the arctangent function:

$$A = tan^{-1}\left(\frac{E_B - E_A}{N_B - N_A}\right) \quad (3)$$

where *E* and *N* represent easting and northing coordinate differences respectively. This method is not only fast and convenient, enabling near real time acquisition of results, but also unaffected by weather conditions, achieving weather independent operation with all weathers capability, thus exhibiting enhanced operational efficiency. Furthermore, the precision of results can be further improved by appropriately extending the observation time.

Among modern observation methods, it is worth mentioning a calculation method for the azimuth remeasuremetnt based on GNSS networks. By relying on the existing GNSS observation network, this method enables azimuth measurement using only a single GNSS receiver (Sugar et al., 2012). In addition, the widespread use of electronic theodolites has also brought great convenience to azimuth observation. An automatic measurement system composed of an electronic theodolite, a GPS receiver, and a laptop with software for processing measurement data can achieve astronomical measurements that meet Grade 1-2 accuracy requirements (Zhao et al., 2003; Zhang et al., 2005; Solarić and Špoljarić, 1992; Špoljarić and Solarić, 2010). Although the accuracy of results obtained through solar observation is relatively low, Solarić et al. (1988, 1990) still achieved

high accuracy based on a large amount of solar observation data, and pointed out that the accuracy is particularly better during sunrise and sunset periods.

2.3 Comparison and Selection

Table 1 presents a brief comparison between the traditional astronomical observation methods and modern observation technologies. Both the methods can achieve high-precision observations, yet each has its own applicable environments. Traditional astronomical observation methods have low reliance on electronic devices and are not affected by electronic signals. However, they are highly dependent on weather conditions, requiring clear skies and good visibility. In contrast, most modern observation technologies rely on GNSS equipment and electronic theodolites. They are easy to operate and can work around the clock, but their performance is poor in environments with insufficient signal coverage or obstructions, and they may be affected by the multipath effect (e.g., increased errors near water surfaces, glass curtain walls, and metal reflective surfaces). According to actual observation data, the maximum GPS positioning error caused by the multipath effect can reach 3.4 cm (Fu, 2004). In high-reflection environments, this error can be as large as 15 cm (Wang, 2000). When the distance from a high-reflection surface is approximately 50 meters or more, the multipath effect can basically be neglected (He, 2010). The two methods are irreplaceable to each other, complementing one another in terms of precision and environmental adaptability. In practical work, measurement methods can be flexibly selected according to the application scenarios.

Table 1: Comparison of Azimuth Measurement Methods

Method	Traditional Astronomical Observation	Modern Observation Technology
Equipment	Theodolite, ephemeris, timer	GNSS receivers, electronic theodolites , data processing software
Limitations	Requires clear skies or visible celestial body	Requires open sky, susceptible to obstructions
Complexity	High (astronomy expertise needed)	Low (automated)
Precision	0.5″ (Polaris based first class measurement)	1″~2″ (ideal conditions)
Applications	Remote areas, military operations, heritage restoration	Engineering survey, UAV navigation, traffic planning
Error Sources	Atmospheric refraction, timing errors, instrument alignment	Multipath effects, ionospheric delay, satellite geometry
Timeliness	Delayed (post processing)	Near real time

In the re-measurement work of azimuth markers at geomagnetic observations in Geomagnetic Network of China, we have chosen the GNSS differential positioning technology. The Geomagnetic Network of China comprises 46 geomagnetic observatoties, and most of them have been in operation for over 10 years. The marker's azimuths of the early-constructed observatories were measured using traditional astronomical methods, and usually obtained during the station construction period. At that time, the observation rooms were not yet roofed, and theodolites could be set up directly on observation pillars to achieve unobstructed visibility of Polaris. Today, however, the rooms have been fully roofed, making it impossible to see the sky from inside. Moreover, the fixed marker pillars outdoors vary in shape (as shown in Fig.3), and are mostly unsuitable

for mounting theodolites on them. Furthermore, traditional astronomical observation is highly dependent on weather conditions. Due to the diverse geographical locations of the observatories, especially those in coastal areas, where cloudy weather is frequent It sometimes often takes several days of waiting for suitable weather to conduct astronomical method, making the measurement process time consuming and inconvenient for arranging remeasurement plans. Therefore, after considering factors such as measurement scenarios, time cost, and operational convenience, the GNSS differential positioning method was selected to complete the remeasurement work.

Figure 3: Different styles of azimuth markers

3 Multi scenarios analysis for azimuth remeasurement

In measurements based on GNSS differential positioning method, due to the varying observational conditions (such as line of sight conditions, terrain features, and surrounding vegetation coverage) across stations, require tailored measurement approaches for different scenarios. The following section discusses five common situations that may be encountered during such remeasurements.

3.1 Scenario I: Flat and clear line of sight

If the path between the observation pillar in the geomagnetic absolute observation room and the azimuth marker is flat and unobstructed, and free from tall vegetation coverage, two GNSS receivers can be deployed along the line of sight (LOS), with sufficient separation distance (for GNSS receivers with a horizontal positioning error of 2 mm, a minimum distance of 200 m between them is required to achieve 2″ level measurement accuracy). Additionally, the targets of both GNSS receivers are visible from the observation pillar. During this remeasurement scenario, the GNSS receivers should be installed along the unobstructed line of sight path while ensuring sufficient distance between them. A high precision theodolite (1″ level) must be used to align the azimuth marker and the two GNSS targets, guaranteeing that the center of the observation pillar, the azimuth marker, and both targets lie on a single straight line.

To achieve collinearity among the four elements, the following operational procedures must be strictly followed: First, set up the theodolite on the observation pillar inside the observation room, and precisely adjust it to ensure the instrument's center aligns perfectly with the pillar's center. Then, perform meticulous theodolite leveling. After leveling, aim at the azimuth marker through the theodolite's telescope, and once the crosshairs coincide exactly with the azimuth marker's center, lock the theodolite's horizontal circle at this position (while keeping the vertical circle freely rotatable). Next, mount the leveling base and GNSS target on a tripod, employing a two-person coordination method—one moving the tripod and the other observing through the theodolite's telescope. Position the tripod within the telescope's field of view, then gradually adjust its placement until the GNSS target infinitely approaches the line defined by the crosshairs and the azimuth marker. Secure the tripod afterward. At this point, adjust the leveling base. After leveling, the GNSS target may deviate from the line, requiring another fine adjustment to realign the marker, followed by re-leveling. This cycle must be repeated multiple times until the base is perfectly level and the GNSS target precisely lies on the line. Only after fulfilling these conditions can the GNSS receiver be mounted on this tripod system. The same procedure is applied to the second tripod. Ultimately, ensure the four elements are rigorously collinear. As shown in Fig.4, images illustrate the alignment process from the observation pillar to the GNSS targets and the azimuth marker. Figure 4(a) demonstrates azimuth marker alignment: After precisely centering the azimuth marker using the telescope crosshairs, the horizontal circle should be locked in place. Figure 4(b) shows initial positioning: The tripod with the GNSS target should be aligned with the sightline formed by the telescope crosshairs and the azimuth marker. Figure 4(c) depicts the first aligned GNSS receiver, while Fig. 4(d) presents the second aligned GNSS receiver and azimuth marker.

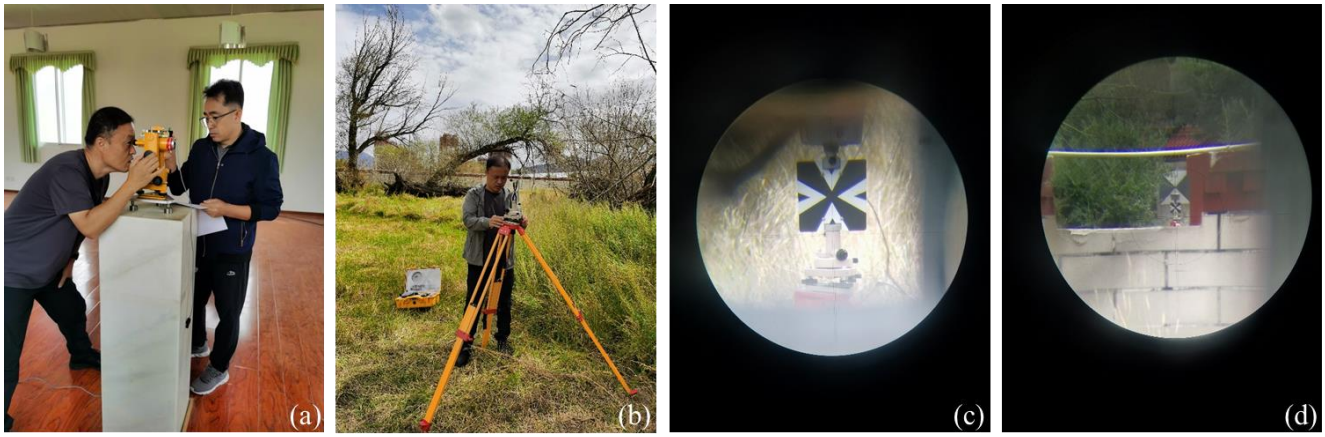

Figure 4: Theodolite alignment to the GNSS targets and the azimuth marker.

Figure 5 illustrates the schematic diagram for calculating the azimuth angle based on this method, where O represents the center of the observation pillar, A and B denote the two GNSS receiver points, M is the azimuth marker, and a_{NM} and a_{GNSS} indicate the azimuth angles of the azimuth marker and the GNSS receiver line, respectively (these symbols retain the same meaning in subsequent schematic diagrams and will not be reiterated in later sections). If the OM distance is sufficiently long to meet measurement requirements, points A and B can be installed between O and M, as shown in Fig. 5(a). However, if the

distance between A and B is too short to satisfy measurement criteria, point B can be relocated beyond marker M to a farther position, as depicted in Fig. 5(b).

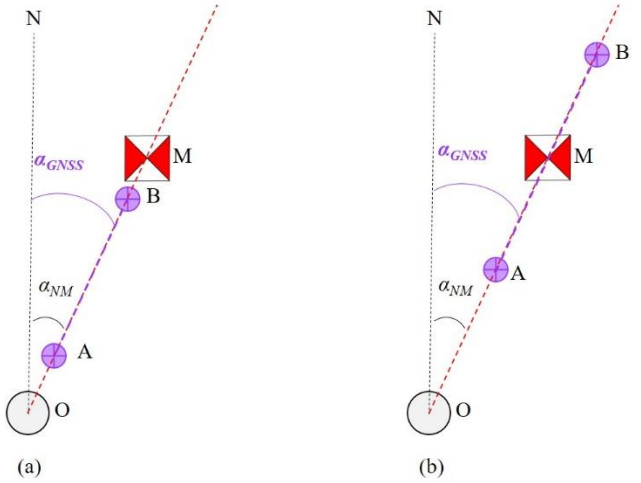

Figure 5: GNSS collinear deployment

As shown in Fig. 5, since points O, A, B, and M lie on the same straight line, the azimuth angle of the OM connection (a_{NM}) is identical to the azimuth angle of the line connecting the two GNSS receiver points A and B (a_{GNSS}). In this scenario, the azimuth angle of the GNSS receiver line is equivalent to that of the azimuth marker:

$$a_{NM} = a_{GNSS} \tag{4}$$

3.2 Scenario II: Alternative clear path available

When there is a clear line of sight between the observation pillar and the azimuth marker, but the path is obstructed by tall vegetation (which may interfere with GNSS satellite signal reception), or the terrain along the path is uneven (preventing visual alignment of targets from the pillar), or the path lacks sufficient distance to deploy two GNSS receivers, an alternative survey line in another direction with clear visibility and sufficient length can be identified. In such scenarios, the GNSS receivers can be deployed along this alternative survey line. By conducting GNSS measurements, the azimuth angle of this line can be determined. Subsequently, using a high precision theodolite (1″ level) to measure the angle between this line and the azimuth marker's path, the azimuth angle of the marker can ultimately be derived. Figure 6 provides a schematic diagram of this measurement method.

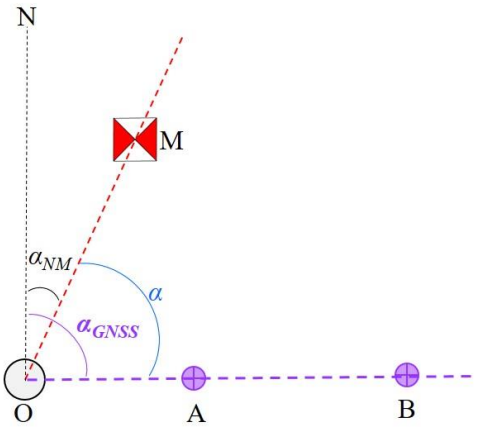

Figure 6: Alternative path GNSS deployment

As shown in Fig. 6, since points O, A, and B are collinear, the GNSS receivers at A and B can measure the azimuth angle of this line (a_{GNSS}). The angle α between the OM line and the collinear line OB can be determined through repeated measurements with a high precision theodolite (1″ level). In this scenarios , the azimuth angle of the observation marker OM (a_{NM}) is derived via the following formula:

$$a_{NM} = a_{GNSS} - a \tag{5}$$

3.3 Scenario III: Single GNSS receiver on LOS

When there is clear line of sight between the observation pillar and the azimuth marker, but insufficient distance or obstructions from tall vegetation prevents to deploy two GNSS receivers along this direction, and only one GNSS receiver is feasible. In such scenario, the following approach can be adopted. One GNSS receiver can be deployed along the path between the observation pillar and the azimuth marker. The second GNSS receiver can be placed on another path with clear mutual visibility to the first GNSS receiver, ensuring the distance meets measurement requirements. Then the azimuth angle of the GNSS baseline can be determined using GNSS differential methods. Subsequently, a high precision theodolite, mounted on the tripod at the first GNSS receiver point, can be used to measure the angle between Point O (or Point M, depending on field setup constraints) and the GNSS target at Point B by conducting repeated measurements. The azimuth angle of the marker can be ultimately calculated using the two angles, as illustrated in Fig. 7.

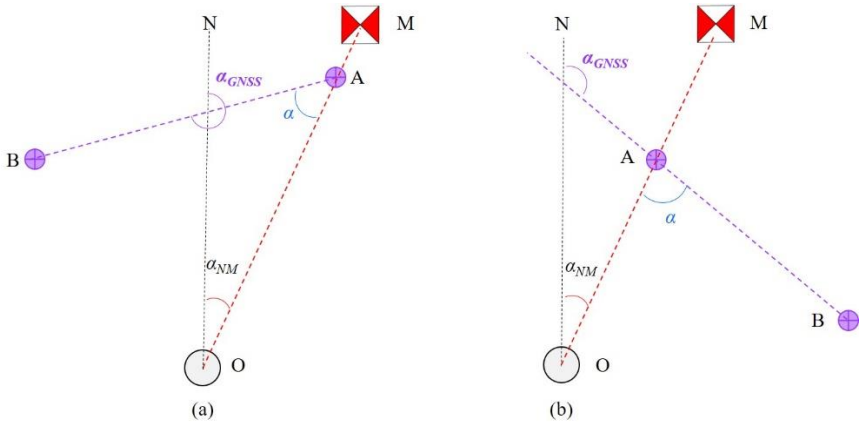

Figure 7: Single GNSS on main path, (a) B is left of A, (b) B is right of A

Figures 7(a) and (b) illustrate the two scenarios where Point B located to the left and right of Point A, respectively. Points O, A, and M are collinear. The azimuth angle of the baseline AB is denoted as a_{GNSS}. The angle between AB and AO is α. The azimuth angle of the marker (a_{NM}) can be calculated as follows:

$$a_{NM} = \begin{cases} a_{GNSS} - 180^{\circ} - a, & (B\ is\ left\ of\ A) \\ a_{GNSS} - (180^{\circ} - a), & (B\ is\ right\ of\ A) \end{cases} \quad (6)$$

3.4 Scenario IV: Single GNSS receiver on alternative path

If no suitable locations are available for deploying GNSS receivers along the direct path between the observation pillar and the azimuth marker, but an alternate point can be identified that maintains line of sight with both the observation pillar and another measurement point meeting distance requirements. The following workflow can be applied in this scenario. First, two GNSS receivers can be deployed at the two measurement points. The azimuth angle of the GNSS baseline connecting the two GNSS receivers can be measured using GNSS differential positioning. Subsequently, a high precision theodolite can be mounted at the GNSS receiver point which is visible to the observation pillar. Through repeated measurements, the angular offset between the second GNSS point and the center of the observation pillar is determined. The theodolite is then relocated to the observation pillar, where repeated measurements are conducted to obtain the angular between the azimuth marker and the visible GNSS point. Finally, the azimuth angle of the azimuth marker is calculated based on the angular relationships derived from these measurements. A schematic diagram of the measurement process is illustrated in Fig. 8.

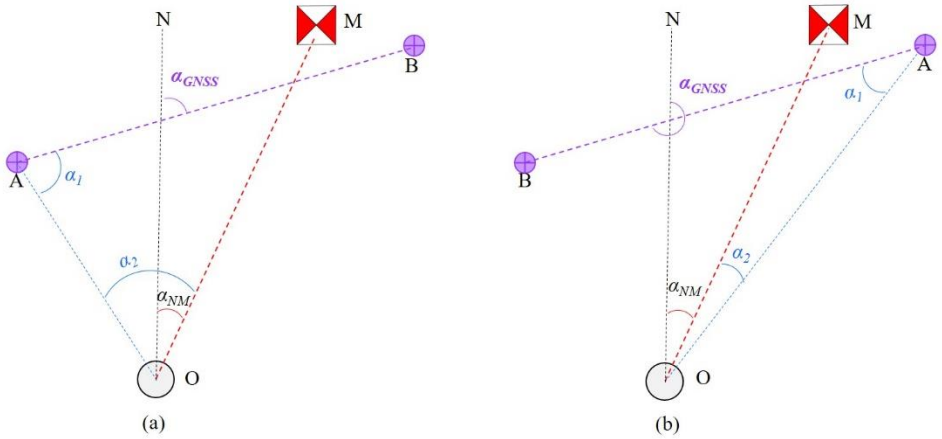

Figure 8. Single point visibility measurement on alternative path, (a) B is right of A, (b) B is left of A

In Fig. 8, Point A is mutually visible to both the center of the observation pillar (O) and measurement point B. Figures 8(a) and (b) depict scenarios where Point B is positioned to the right and left of Point A, respectively. Here, a_{GNSS} denotes the azimuth angle measured by GNSS differential positioning, while α_1 and α_2 represent the angular offsets observed at Point A and the observation pillar. Based on the angular relationships illustrated in the figures, the azimuth angle of the azimuth marker is calculated as follows:

$$a_{NM} = \begin{cases} (a_{GNSS} - 180^\circ) - a_1 - a_2, & (B\ is\ left\ of\ A) \\ a_{GNSS} - (180^\circ - a_1 - a_2), & (B\ is\ right\ of\ A) \end{cases} \quad (7)$$

3.5 Scenario V: No GNSS deployment feasibility

If none of the preceding scenarios are applicable (i.e., no GNSS compatible locations exist within the line of sight range of the observation pillar in the observation room), but an auxiliary point can be identified that is both mutually visible to the observation pillar and aligned with a survey line that meets GNSS deployment requirements. Then the remeasurements can be completed rely on the auxiliary mutually visible point.

Most geomagnetic observatories were equipped with calibration huts containing an observation pillar. This pillar was designed to maintain mutual visibility with the observation pillar in observation room and to offer clear sightlines to its surroundings (if Polaris could be observed from this pillar, astronomical azimuth methods could theoretically be applied, though this is not discussed here). If a specific direction near the pillar provides unobstructed visibility and meets the requirements for deploying two GNSS receivers, the pillar can serve as an auxiliary reference point. If such a pillar is not available at the observatory, a tripod can be set up at the location to act as a temporary auxiliary point.

In this scenario, a high precision theodolite is set up at the auxiliary point (either the observation pillar in the calibration hut or a tripod mounted location). The theodolite is aligned to ensure that the two GNSS measurement points lie on the same survey line. Through repeated measurements, the angular a_1 between the target marker of either GNSS and the center O (marked by a fine needle secured with clay) of the observation pillar in the observation room is determined. Subsequently, the

high precision theodolite is relocated to the observation pillar inside the observation room, where repeated measurements the angular a_2 between the azimuth marker and the center P of the auxiliary point. Finally, by integrating the results from GNSS differential positioning, the azimuth angle of the azimuth marker can be calculated. Figure 9 illustrates a schematic diagram of this measurement method.

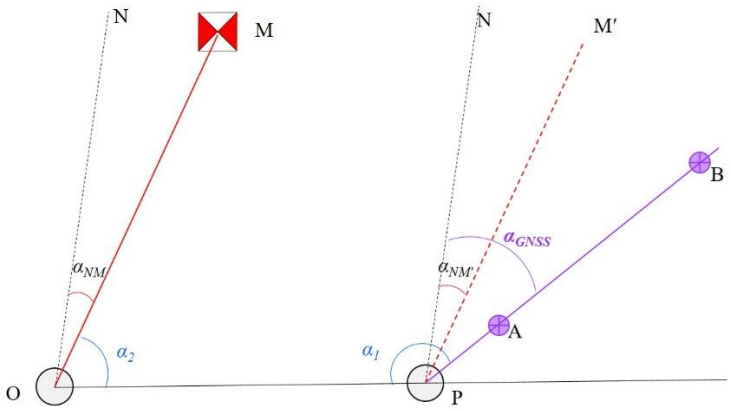

Figure 9. Indirect measurement via auxiliary point.

In Fig. 9, point P represents the center of the auxiliary measurement point (observation pillar or tripod setup), and PM' is the parallel line to OM. Thus, the azimuth angle a_{NM} equals $a_{NM'}$. From the angular relationships shown in the figure, the azimuth angle of the marker can be derived as:

$$a_{NM} = a_{GNSS} - (a_1 + a_2 - 180^{\circ}) \quad (8)$$

4 Multi scenarios case studies in azimuth remeasurement

The previous text analyzed five potential scenarios for azimuth remeasurement and provided corresponding measurement solutions. Based on these scenarios, we have preliminarily initiated remeasurements at stations with long standing azimuth markers and obtained initial results. Currently, azimuth remeasurements have been completed at three stations: Hongshan Geomagnetic Observatory, Quanzhou Geomagnetic Observatory, and Yulin Geomagnetic Observatory.

Hongshan Geomagnetic Observatory, located in the North China Plain, started its previous azimuth marker in 2003 (22 years ago); the path between its observation pillar and azimuth marker features flat terrain with a completely unobstructed line of sight, satisfying Scenario I conditions, hence Scenario I methodology was adopted. Quanzhou Geomagnetic Observatory in southeastern China's hilly terrain has its azimuth marker engraved on bedrock, dating back to 2007 (18 years ago); although the path is complex, two measurement point meeting Scenario I requirements can be identified, so Scenario I was applied. Yulin Geomagnetic Observatory, located in the suburban area of Yulin, northwestern China, had its original primary azimuth marker destroyed. However, before its destruction, the azimuth angle was transferred to the rooftop of a distant building and has been in use since 2009 (16 years ago). Due to multiple buildings and tall trees obstructing the path, measurements using

Scenario I were unfeasible. Fortunately, an alternative survey line meeting Scenario II requirements was identified from the opposite side of the observation room, enabling azimuth remeasurement via Scenario II. Additionally, Scenario IV methodology was also attempted in Yulin observatory. Detailed results for all three observatories are presented in Table 2.

Table 2. Comparison of remeasured and original azimuth angles

Observatory	Scenario	Pillar No.	Remeasured (GNSS)		Original (Astronomy)	Difference
			Azimuth	Standard deviation	Azimuth	
Hongshan	I	1#	1° 31′ 55.8″	±2.1″	1° 31′ 52.2″	3.6″
		2#	2° 22′ 10.8″	±1.6″	2° 22′ 9.6″	1.2″
Quanzhou	I	1#	179° 46′ 37.9″	±0.7″	179° 46′ 28.6″	9.3″
		5#	178° 30′ 34.4″	±0.8″	178° 30′ 25.6″	8.8″
Yulin	II	1#	354° 49′ 40.2″	±0.7″	354° 49′ 31.2″	9.0″
	IV	1#	354° 48′ 49.3″	±0.7″		41.9″

In the azimuth remeasurement work at these three geomagnetic observatories, we uniformly used the GNSS equipment with the rapid static horizontal accuracy 2.5mm+0.5ppm RMS, employed the Zeiss Theo 010B theodolite with an angular measurement accuracy of 1^{cc} ($0.324''$), war used for collinearity alignment and angle measurement. Additionally, three sets of data were collected for each GNSS survey line, and the mean value and standard deviation are presented in Table 2. Most of the differences between the re-measured azimuths and the original astronomical azimuths are within the range of 0-9″, that is consistent with theoretical expectations.

It should be noted that the azimuth obtained by the astronomical observation method is referenced the plumb line, while the azimuth obtained by the geodetic method (derive from the GNSS method) is based on the ellipsoidal normal. So the vertical deflection introduces systematic error to the azimuths (Vittuari et al., 2016). Account for the influence of vertical deflection, it is necessary to apply the Laplace azimuth equation (9) to convert the astronomical azimuth to the ellipsoidal normal based azimuth (Torge, 2001).

$$a - A = -\eta \tan\varphi + \frac{\eta \cos\alpha - \xi \sin\alpha}{\tan\zeta} \tag{9}$$

Where A is the azimuth determined by astronomic observation and referred to the plumb line, a is the azimuth referred to the ellipsoid normal, ζ is the ellipsoidal zenith-distance to the reference mark, η and ξ are the components of the deflection of the vertical: $\xi = \Phi - \varphi$ and $\eta = (\Lambda - \lambda)\cos\varphi$. They can be calculated by the astronomic coordinates (Φ, Λ) and the ellipsoidal coordinates (φ, λ). Due to the lack of astronomical latitude Φ and longitude Λ values for the measured points, it is temporarily impossible to conduct this calculation. However, previous measurement results can serve as reference for evaluation. For example, Šugar et al. (2012) compared azimuths obtained from astronomical methods and GNSS measurements, finding an average difference of 0.8″, and the standard deviation of the astronomical azimuth was ±2.6″. Based on 14 astronomical

observations and comparative experiments with GNSS, Wang et al. (2001) reported that the differences between the two methods mostly ranged between 0–3″, with a maximum difference of up to 4.5″. Therefore, when considering systematic deviations between astronomical and GNSS methods, positioning errors, sighting alignment errors, and other factors, a discrepancy of 0–9″ is within expected limits. Furthermore, in terms of the accuracy requirement for azimuth in absolute geomagnetic observation (0.1′), a variation of 0–9″ over several decades is considered acceptable. Thus, it can be concluded that no significant displacement has occurred at the observation markers.

5 Conclusions and discussion

This paper briefly compares two methods for measuring azimuth markers at geomagnetic observatories and proposes five applicable remeasurement scenarios based on GNSS differential positioning, comprehensively covering all remeasurement challenges. Comparative analysis reveals:

Scenario I requires only GNSS receiver alignment (ensuring collinear points), simplifying operations without angular measurements or conversions, thus introducing no additional errors beyond four points alignment inaccuracies. Scenarios II and III necessitate measuring one angle (beyond alignment), introducing single error sources. However, Scenario II performs this measurement on more stable observation pillars, while Scenario III uses tripods, making Scenario II superior. Scenarios IV and V require measuring two angles (introducing dual errors), with one typically tripod based. If Scenario V employs a stable observation pillar as an auxiliary point, it outperforms Scenario IV. Consequently, based on the principle of 'one more measurement, one more error introduced', in order to minimize the introduction of errors, the priority order of measurement schemes for remeasurement is as follows: Scenario I (optimal) > Scenario II > Scenario III > Scenario V (with fixed pillar) > Scenario IV.

Field measurements at three observatories using Scenarios I and II confirm the feasibility of these remeasurement methods. However, in the Scenario IV test at Yulin observatory, a significant deviation (>40″) was observed between the measured and original results. Two primary factors may contribute to this result. The first one is the insufficient GNSS baseline length. Despite the RMSE of three measurement sets remained stable at 0.7″, the short distance between two GNSS points (about 60 m) and the maximum horizontal error (about 2.5 mm) may introduce the potential angular error of up to 8.6″. The second one is the theodolite setup error. In this scenario, the theodolite needs to be installed on the tripod at point A, as shown in Fig. 8(b). During angle measurement process, a centering offset was detected on the tripod. After re-centering, a change of 10.8″ occurred. This underscores the necessity of adequate baseline distances and highlights the need for further analysis of tripod measurement error characteristics. Nevertheless, we detected minor azimuth shifts—though numerically small, these findings enhance data accuracy assurance for observatory operations, validating the significance of this work.

Remeasurements show minimal azimuthal changes at all three observatories. Quanzhou's marker is engraved on bedrock; Hongshan's marker is mounted on a pillar with a stable foundation on level ground; Yulin's original mark was destroyed, and

its marker relocated to a distant rooftop (relatively stable but weather vulnerable and not recommended for permanent markers). These cases highlight that marker stability of azimuth markers is crucial.

Data availability

All raw data can be provided by the corresponding authors upon request.

Author contribution

YH and XZ initiated the study. SZ and QL designed the analysis methods. FY, SH and PG carried them out. JZ provided photos of the azimuth markers. YH prepared the manuscript with contributions from all coauthors.

Competing Interests

The authors have no competing interests to declare.

Acknowledgements

We express our gratitude to the colleagues at Hongshan geomagnetic observatory, Quanzhou geomagnetic observatory, and Yulin geomagnetic observatory for their assistance during the azimuth remeasurement process, which enabled the smooth completion of the survey work.

Funding Information

Supported by National Key R&D Program of China (2023YFC3007404; 2018YFC1503505); National Natural Science Foundation of China (42374092).

References

Bracke, S., INTERMAGNET Operations Committee and Executive Council: INTERMAGNET Technical Reference Manual, Version 5.2.0, https://tech-man.intermagnet.org/_/downloads/en/stable/pdf/, Last accessed 20 May 2025.

Cheng P.G., Li J.P. and Yu X.H.: Software of analytic method for determining astronomical azimuth, Engineering of Surveying and Mapping,5(4):44-50,1996.

China Earthquake Administration (CEA): Specification for the construction of seismic station: Geomagnetic station (in Chinese). DB/T 9–2004. Beijing: Seismological Publishing House. 2004.

China Earthquake Administration (CEA): Technical specifications for digital seismic and precursor observation: Electromagnetic Observation (Trial Implementation) [M]. Beijing: Seismological Publishing House, 11-16, 2001.

Fu P.Y.: The analysis of multipath error of GPS measuring with practical data, Chinese Journal of Scientific Instrument, 25(4): 748-749, 2004.

He Y.L.: The study of multi-path effects on high precision GPS surveying, Engineering of Surveying and Mapping, 19(1): 35-38, 2010.

Jankowski, J., and Sucksdorff, C.: Absolute magnetic measurement, in: Guide for magnetic measurements and observatory practice, IAGA, Warszawa, Poland, 87–102, 1996.

Khanzadyan M. A. and Mazurkevich A.V.: Development of a method for measuring the astronomical azimuth using an electronic total station. E3S Web of Conferences, 310(03007), https://doi.org/10.1051/e3sconf/202131003007, 2021.

Li S.M., Wang G.G. and Shen Z.F.: Theory, method and application of positioning and navigation of geomagnetic field, Gnss World of China, 2023, 48(6): 42-51. DOI: 10.12265/j.gnss.2023141,2023.

Li Q.H., Xin C.J., Xu K.S., Shu L. and Gao H.H.: Application of differential GPS to the geographic azimuth measurement in China geomagnetic field monitoring network, China Earthquake Engineering Journal, 37(3):863-866, DOI:10.3969/ji.ssn.1000-0844.2015.03.0862, 2015.

Lin Y, Sun J.J. and Yang X.: A review of the principles and methods of geomagnetic navigation and positioning technology, Gnss World of China, 48(6): 32-41, DOI: 10.12265/j.gnss.2023134, 2023.

Liu X.J., Zhegn Y. and Li C.H.: Precise determination of astronomical azimuth by hour angle method of multiple meridian stars. ACTA ASTRONOMICA SINICA,61(3):1-10, doi:10.15940/j.cnki.0001-5245.2020.03.008, 2020.

Lu Y., Wei D.Y., Ji X.C. and Yuan H.: Review of geomagnetic positioning method, Navigation Positioning& Timing, 9(2):118-130, doi:10.19306/j.cnki.2095-8110.2022.02.015, 2022.

Ma H.B.: Deriviation of formulas for astronomical azimuth determination and approach to the method, Journal of Shenyang Institute of Gold Technology, 14(3):331-336,1995.

Shi J.G.: Surveying data transmission method in drilling, Petroleum Drilling Techniques, 36(4):15-17, 2008.

State Bureau of Quality and Technical Supervision (SBQTS): Specification for the geodetic astronomy, GB/T 17943-2000, https://openstd.samr.gov.cn (last access: 26 May 2025), 2000.

St-Louis, B., INTERMAGNET Operations Committee and INTERMAGNET Executive Council: INTERMAGNET Technical Reference Manual, Version 5.1.1, (INTERMAGNET), Potsdam: GFZ Data Services, 134 p. https://doi.org/10.48440/INTERMAGNET.2024.001, Last accessed 20 May 2025.

Solarić N. and Špoljarić D.: Accuracy of the automatic grid azimuth determination by observing the Sun using Kern E2 theodolite. Surveying and Mapping, USA, 48(1):19-28, 1988.

Solarić N. and Špoljarić D.: Accuracy of the automatic astronomical azimuth determination by Polaris with Leica-Kern E2 electronic theodolite. Surveying and Land Information System, (2):80-85, 1992.

Solarić N., Špoljarić D. and Nogić Č.: Analysis of the accuracy of the automatic azimuth determination by measuring zenith distances of star with electronic theodolite Kern E2. Hvar Obs. Bull., 14:1-14, 1990.

Špoljarić D. and Solarić N.: Automation of astrogeodetic measurements. Proceedings of the 10th International Multidisciplinary Scientific Geoconference SGEM 2010, I:837-844, 2010.

Šugar D., Brkić M. and Špoljarić D.: Comparison of the reference mark azimuth determination methods. Annals of Geophysics, 55(6):1071-1083, doi: 10.4401/ag-5405, 2012.

Torge W.: Geodesy. Walter de Gruyter, Berlin/New York, 2001.

Vittuari L., Tini M. A., Sarti P., Serantoni E., Borghi A., Negusini M. and Guillaume S.: A comparative study of the applied methods for estimating deflection of the vertical in terrestrial geodetic measurements. Sensors, 16(4):565, doi:10.3390/s16040565, 2016.

Wang J.B.: Discussion on GPS azimuth system conversion and its accuracy, Beijing Surveying and Mapping, (1): 24-27, 2001.

Wang X.Q.: The effects of multipath errors on GPS surveying, Crustal Deformation and Earthquake, 20(1): 56-59, 2000.

Wang Z. Y., Jiang H. and Hou Y.J.: Azimuth angle measurement of Dalian geomagnetic station, Azim uth angle m easurem ent of Dalian Geom agnetic Station, Seismological and Geomagnetic Observation and Research, 35(5/6):120-123, doi:10.3969/j.issn.1003-3246.2014.05/06.023.2014.

Xu X.G., Shang X.Q. and Zhou J.P.: Measurement of astronomic azimuth angle in Jinghai station and its quality evaluation, Northwestern Seismological Journal, 25(3): 281-285,2003.

Yang F. X., Yang X., Zhang X. Y. and Huang J. M.: Azimuth suervey of Urumqi geomagnetic station marker, Inland Earthquake,22(4):306-313,2008.

Yin W.T.: Obtaining the azimuth with GPS, Geomatics & SpatialInformationTechnology,31(1):120-126, 2008.

Yu J.K., Zhao R.R. and Ren Y.C.: Directional azimuth of GNSS calculation method, Journal of Navigation and Positioning, 6(1):120-122, doi:10.16547/j.cnki.10-1096.20180122, 2018.

Zhang C., Zheng Y., Meng F.Y. and Chang L.L.: Measure astronomical azimuth using GPS and electronic theodolite, Journal of Information Engineering University, 6(2): 96-99, 2005.

Zhang H.B., Lian Q., Kang C.K. and Zhou J.: uantitative analysis of the relationship between geomagnetic anomaly and geological structure, Geological and Mineral Surveying and Mapping,7(6): DOI:10.12238/gmsm.v7i6.1847, 2024a.

Zhang, S. Q., Fu, C. H., He, Y. F., Yang, D. M., Li, Q., Zhao, X. D., and Wang, J. J.: Quality control of observation data by the Geomagnetic Network of China, Data Science Journal, 15, 1–12, DOI:http://dx.doi.org/10.5334/dsj-2016-015, 2016.

Zhang, S. Q., Fu, C. H., Zhao, X. D., Zhang, X. X., He, Y. F., Li, Q., Chen, J., Wang, J. J., and Zhao, Q.: Strategies in the Quality Assurance of Geomagnetic Observation Data in China, Data Science Journal, 23, 1–11, DOI: https://doi.org/10.5334/dsj2024-009, 2024b.

Zhao L.C. and Xiong Y.: Azimuth of Polaris application of new techniques to surveying astronomic, Journal of Geomatics, 28(3): 37-39, 2003.

Zhou J.P., Huang W.B., Cheng A.L., et al.: Azimuth measurement and error analysis at Beijing geomagnetic observatory, Seismological and Geomagnetic Observation and Research,18(6):73-79,1997.

Zhou Y. T., Li Y. G. and Shang Q. F.: Study on the calibration method for the difference GPS direction, Journal of Astronautic Metrology and Measurement, 29(4):50-53, 2009.